JOURNAL OF GUIDANCE, CONTROL, AND DYNAMICS
Vol. 40, No. 3, March 2017

Engineering Notes

Instantaneous Quadratic Power-Optimal Attitude Tracking with N Control Moment Gyroscopes

Daniel P. Lubey* and Hanspeter Schaub†
University of Colorado, Boulder, Colorado 80309

DOI: 10.2514/1.G001659

Nomenclature

$\hat{g}_{s,i}$; $\hat{g}_{t,i}$; $\hat{g}_{g,i}$	=	unit vectors defining the ith CMG's spin s, transverse t, and gimbal g directions
$[I_{G_i}]$	=	inertia tensor of the ith gimbal about its center of mass, kg · m^2
$[I_S]$	=	spacecraft inertia tensor including all rigid components and static offsets from each control moment gyroscope, kg · m^2
$[I_{W_i}]$	=	inertia tensor of ith wheel about its center of mass, kg · m^2
K	=	scalar control gain that drives attitude toward reference, N · m
$K_{\dot{\gamma}}$	=	scalar control gain that drives gimbal rate toward desired value, s^{-1}
$\boldsymbol{L}$	=	external torque vector, N · m
$\hat{n}$	=	unit vector defining null space of control matrix $[D]$
$[P]$	=	matrix control gain that drives angular velocity toward reference, N · m · s
$u_{g,i}$	=	torque supplied by ith control moment gyroscope along its gimbal axis, N · m
$u_{s,i}$	=	torque supplied by ith control moment gyroscope along its spin axis, N · m
$\boldsymbol{\beta}$	=	quaternion defining orientation of spacecraft body frame with respect to inertial frame
γ_i	=	gimbal angle of ith control moment gyroscope, rad
$\dot{\gamma}_{d,i}$	=	desired gimbal rate of ith control moment gyroscope, rad/s
$\dot{\gamma}_{\max}$	=	maximum allowed gimbal rate magnitude, rad/s
$\delta\boldsymbol{\sigma}$	=	modified Rodriguez parameter defining orientation of body frame with respect to reference frame
$\delta\boldsymbol{\omega}$	=	angular velocity of body frame with respect to reference frame, rad/s
$\boldsymbol{\lambda}$	=	Lagrange multiplier used to enforce equality constraint
μ	=	Lagrange multiplier used to enforce inequality constraint
τ	=	scaling parameter used to define null space motion
Ω_i	=	wheel speed of ith control moment gyroscope, rad/s
$\boldsymbol{\omega}_{B/N}$	=	angular velocity of body frame with respect to inertial frame, rad/s
$\boldsymbol{\omega}_r$	=	angular velocity of reference frame with respect to inertial frame, rad/s

Received 25 August 2015; revision received 11 June 2016; accepted for publication 7 August 2016; published online 9 December 2016.

*Graduate Research Assistant, Aerospace Engineering Sciences; daniel.lubey@colorado.edu.

†Professor, Aerospace Engineering Sciences; hanspeter.schaub@colorado.edu.

I. Introduction

ATTITUDE control aboard a spacecraft is typically done in one of two ways: 1) using external forces to torque the vehicle into a desired orientation (e.g., thrusters, magnetic torque rods, etc.) and 2) using internal torques to reorient the system [e.g., reactions Wheels (RWs), control moment gyroscopes (CMGs), etc.]. In the latter case, internal power is used to operate these momentum management devices. Spacecraft power must be managed properly and preserved, because missions can only persist as long as a power source is available. As such, a minimum power policy for operating these devices is desired. Optimization methods can also be quite computationally intense, which is not always suitable for onboard implementation. As such, we seek control methods that are computationally simple as well as being power minimizing.

Much of the work in power optimizing attitude control has focused on RW systems. This work includes that by Schaub and Lappas [1], who developed a null-space-based method for infinite-horizon instantaneous L_2 power-optimal control; Blenden and Schaub [2], who investigated flywheel capabilities for energy storage while controlling attitude; and Dueri et al. [3], who took advantage of friction in these systems to aid in power optimization. CMGs provide an effective means to reorient a spacecraft for large and small missions alike [4,5], and especially for missions that cannot include a propellant system, it provides the controllability necessary to accomplish mission goals. As such, power-optimal attitude control using CMGs is of considerable interest. Research in this field to date includes the work by Leve et al. [6], who addressed the problem by optimizing the orientations of the CMGs within the spacecraft; DeVon et al. [7], who approached the problem from a passivity formulation using variable speed control moment gyroscopes (VSCMGs); and Carpenter [8], who specifically addressed instantaneous power optimization for CMG systems, but this application is for systems with robotic linkages rather than spacecraft attitude control. The existing literature only covers a portion of the larger problem of power-optimal attitude control with CMGs.

The unexplored problem addressed in this paper is instantaneous infinite-horizon attitude control of rigid spacecraft with redundant CMGs ($N > 3$). Section II reviews the equations of motion for a spacecraft with N CMG devices along with a control law that asymptotically tracks a given attitude reference motion. Section III develops the new power-optimal control tracking law, which is the primary contribution of this paper. Section IV provides a sample attitude-tracking simulation in which the minimum norm tracking control law is compared against the power-optimal solution that is derived in this paper. Finally, Sec. V provides some concluding remarks.

II. Dynamics and Control of N CMG Systems

This section focuses on the equations of motion for a system with N CMGs and an associated reference attitude-tracking control law. These are defined in the following subsections.

A. N CMG Equations of Motion

A full derivation of these equations of motion is provided in [9] (Chap. 4); thus, we will focus on the final form of the equations and the notation that will be used throughout this paper.

Generally, four frames are used to define the system: 1) the inertial frame N; 2) the principal body frame B, which stays aligned with the spacecraft's principal axes; 3) the gimbal frames G, which stay aligned with their respective CMG as it gimbals; and 4) the wheel frames W, which stay aligned with their respective wheel as it rotates. Each CMG has its own G and W frames, but the spacecraft has only one body frame of interest B.

Summing all sources of angular momentum, taking the inertial time derivative, and setting this equal to the amount of external torque in the system, the attitude equations of motion for the spacecraft body frame with respect to the inertial frame are obtained as follows ([9] Chap. 4):

$$[I]\dot{\boldsymbol{\omega}} + A_{\ddot{\gamma}}\ddot{\boldsymbol{\gamma}} = -\boldsymbol{\omega} \times [I]\boldsymbol{\omega} - A_{\dot{\gamma}}\dot{\boldsymbol{\gamma}} - A_{\Omega}\boldsymbol{\Omega} + \boldsymbol{L} \tag{1}$$

$$A_{\ddot{\gamma}} = G_g\langle \boldsymbol{J}_g \rangle \tag{2}$$

$$A_{\dot{\gamma}} = G_s(\langle \boldsymbol{J}_s \rangle - \langle \boldsymbol{J}_t \rangle + \langle \boldsymbol{J}_g \rangle)\langle \boldsymbol{\omega}_t \rangle + G_t[(\langle \boldsymbol{J}_s \rangle - \langle \boldsymbol{J}_t \rangle - \langle \boldsymbol{J}_g \rangle)\langle \boldsymbol{\omega}_s \rangle + \langle \boldsymbol{J}_s \rangle\langle \boldsymbol{\Omega} \rangle] \tag{3}$$

$$A_{\Omega} = G_t\langle \boldsymbol{J}_s \rangle\langle \boldsymbol{\omega}_g \rangle - G_g\langle \boldsymbol{J}_s \rangle\langle \boldsymbol{\omega}_t \rangle \tag{4}$$

$$[I] = [I_S] + \sum_{i=1}^{N} [J_i] \tag{5}$$

$$[J_i] = [I_{Gi}] + [I_{Wi}] \tag{6}$$

$$G_s = [\,\hat{g}_{s,1} \quad \ldots \quad \hat{g}_{s,N}\,] \tag{7}$$

$$G_t = [\,\hat{g}_{t,1} \quad \ldots \quad \hat{g}_{t,N}\,] \tag{8}$$

$$G_g = [\,\hat{g}_{g,1} \quad \ldots \quad \hat{g}_{g,N}\,] \tag{9}$$

$$[\,\boldsymbol{\omega}_s^T \quad \boldsymbol{\omega}_t^T \quad \boldsymbol{\omega}_g^T\,]^T = [\,G_s \quad G_t \quad G_g\,]^T\boldsymbol{\omega}_{B/N} \tag{10}$$

In the previous expressions (and throughout the remainder of this paper), the following notational definitions are used:

$$\boldsymbol{x} = [\,x_1 \quad \ldots \quad x_N\,]^T \tag{11}$$

$$\langle \boldsymbol{x} \rangle = \mathrm{diag}(x_i) \tag{12}$$

This puts the equations in a compact vector form by assembling CMG values ($J_{s,i}$, $J_{t,i}$, $J_{g,i}$, Ω_i, γ_i, $\dot{\gamma}_i$, and $\ddot{\gamma}_i$) into vector and matrix forms.

These equations make the assumption that the wheel spin axis inertia dominates the gimbal spin axis inertia. Assuming the user evaluates these equations in the body frame B, the gimbal frame unit vectors must also be expressed in the body frame, and the $[J_i]$ must be rotated to the body frame in Eq. (5). The wheel is also assumed to be symmetric about its rotation axis so that the same inertia value may be used for the transverse and gimbal directions. It should be noted that the gimbal axes are fixed with respect to the body frame by definition, and the other spin and transverse axes are defined simply by the gimbal angle as defined as follows [9]:

$$\hat{g}_{s,i}(t) = \cos[\gamma_i(t) - \gamma_i(t_0)]\hat{g}_{s,i}(t_0) + \sin[\gamma_i(t) - \gamma_i(t_0)]\hat{g}_{t,i}(t_0) \tag{13a}$$

$$\hat{g}_{t,i}(t) = -\sin[\gamma_i(t) - \gamma_i(t_0)]\hat{g}_{s,i}(t_0) + \cos[\gamma_i(t) - \gamma_i(t_0)]\hat{g}_{t,i}(t_0) \tag{13b}$$

$$\hat{g}_{g,i}(t) = \hat{g}_{g,i}(t_0) \tag{13c}$$

To this point, we have only addressed the attitude dynamics of the spacecraft. Now, we must address the CMG states, which will be controlled via a gimbal torque as defined in the following for each CMG using the vector notation of Eq. (11):

$$C_{\dot{\omega}}\dot{\boldsymbol{\omega}} + C_{\ddot{\gamma}}\ddot{\boldsymbol{\gamma}} = \boldsymbol{u}_g + [\langle \boldsymbol{J}_s - \boldsymbol{J}_t \rangle\langle \boldsymbol{\omega}_s \rangle + \langle \boldsymbol{J}_s \rangle\langle \boldsymbol{\Omega} \rangle]\boldsymbol{\omega}_t \tag{14}$$

$$C_{\dot{\omega}} = \langle \boldsymbol{J}_g \rangle G_g^T \tag{15}$$

$$C_{\ddot{\gamma}} = \langle \boldsymbol{J}_g \rangle \tag{16}$$

It should be noted that gimbal accelerations and gimbal rates are sufficient to define the equations of motion for the CMGs, but the equations presented previously allow for a more realistic implementation since gimbal torques are commanded rather than gimbal accelerations. Spin torques are designed to maintain a constant wheel rate, and transverse torques are enforced structurally by the gimbal frame to maintain a fixed gimbal direction (with respect to the body).

The system as defined has $3 + 2N$ states: 1) three for angular rate of the spacecraft, 2) N gimbal angles, and 3) N gimbal rates. A full state vector is defined as

$$\boldsymbol{Z} = [\,\boldsymbol{\omega}^T \quad \boldsymbol{\gamma}^T \quad \dot{\boldsymbol{\gamma}}^T\,]^T \tag{17}$$

Using this full state notation, we define the combined equations of motion in a compact matrix form as

$$[M]\dot{\boldsymbol{Z}} = \boldsymbol{F} \tag{18}$$

$$[M] = \begin{bmatrix} [I] & 0_{3\times N} & A_{\ddot{\gamma}} \\ 0_{3\times N} & I_{N\times N} & 0_{N\times N} \\ C_{\dot{\omega}} & 0_{N\times N} & C_{\ddot{\gamma}} \end{bmatrix} \tag{19}$$

$$\boldsymbol{F} = \begin{bmatrix} -\boldsymbol{\omega} \times [I]\boldsymbol{\omega} - A_{\dot{\gamma}}\dot{\boldsymbol{\gamma}} - A_{\Omega}\boldsymbol{\Omega} + \boldsymbol{L} \\ \dot{\boldsymbol{\gamma}} \\ \boldsymbol{u}_g + [\langle \boldsymbol{J}_s - \boldsymbol{J}_t \rangle\langle \boldsymbol{\omega}_s \rangle + \langle \boldsymbol{J}_s \rangle\langle \boldsymbol{\Omega} \rangle]\boldsymbol{\omega}_t \end{bmatrix} \tag{20}$$

In this notation, $I_{N\times N}$ is the $N \times N$ identity matrix, and $0_{N\times N}$ is the $N \times N$ zero matrix. Additionally, an attitude description is necessary to fully describe the system for a tracking problem (such as presented in this paper). The numerical simulations presented here integrate in Euler parameters and use modified Rodriguez parameters (MRPs)

for the tracking control, but any attitude description could be implemented.

B. Reference Attitude-Tracking Control Law

Having defined the natural equations of motion, we now define a reference attitude-tracking control using the gimbal rates as control variables (though the gimbal torques are the actual implemented control). The control summarized in this section is the same as developed by Schaub and Lappas [1], and thus only the results are reported here. The power-optimal guidance strategy developed in this paper is not tied to this particular attitude control law. Rather, any CMG-attitude control strategy will lead to the same gimbal rate control constraint formulation.

This tracking control is obtained using Lyapunov analysis. The positive definite, radially unbounded, and continuously differentiable Lyapunov function along with its designed negative semidefinite time derivative is shown in the following to provide a reference for the control gains involved [1,9]:

$$V(\delta\boldsymbol{\sigma}, \delta\boldsymbol{\omega}) = \frac{1}{2}\delta\boldsymbol{\omega}^T[I]\delta\boldsymbol{\omega} + 2K\ln(1+\delta\boldsymbol{\sigma}^T\delta\boldsymbol{\sigma})$$
$$\dot{V}(\delta\boldsymbol{\sigma}, \delta\boldsymbol{\omega}) = -\delta\boldsymbol{\omega}^T[P]\delta\boldsymbol{\omega} \tag{21}$$

Although the rate is only negative semidefinite, application of the LaSalle invariance principle [10] or the Mukherjee-Chen theorem [11] confirms that the resulting control is globally asymptotically stable. The resulting control strategy is summarized in the following:

$$[D]\dot{\boldsymbol{\gamma}} + [B]\ddot{\boldsymbol{\gamma}} = \boldsymbol{L}_r \tag{22}$$

$$\begin{aligned}
[B] &= G_g\langle \boldsymbol{J}_g\rangle \\
[D] &= [D1] - [D2] + [D3] + [D4] \\
[D1] &= \left(G_t\left(\langle\boldsymbol{\Omega}\rangle + \frac{1}{2}\langle\boldsymbol{\omega}_s\rangle\right) + \frac{1}{2}G_s\langle\boldsymbol{\omega}_t\rangle\right)\langle\boldsymbol{J}_s\rangle \\
[D2] &= \frac{1}{2}(G_s\langle\boldsymbol{\omega}_t\rangle + G_t\langle\boldsymbol{\omega}_s\rangle)\langle\boldsymbol{J}_t\rangle \\
[D3] &= (G_s\langle\boldsymbol{\omega}_t\rangle - G_t\langle\boldsymbol{\omega}_s\rangle)\langle\boldsymbol{J}_t\rangle \\
[D4] &= \frac{1}{2}(G_s\langle G_t^T\boldsymbol{\omega}_r\rangle + G_t\langle G_s^T\boldsymbol{\omega}_r\rangle)(\langle\boldsymbol{J}_s\rangle - \langle\boldsymbol{J}_t\rangle)
\end{aligned} \tag{23}$$

$$\begin{aligned}
\boldsymbol{L}_r = {} & K\delta\boldsymbol{\sigma} + [P]\delta\boldsymbol{\omega} + \boldsymbol{L} - [\tilde{\boldsymbol{\omega}}][I]\boldsymbol{\omega} - [I](\dot{\boldsymbol{\omega}}_r - [\tilde{\boldsymbol{\omega}}]\boldsymbol{\omega}_r) \\
& - (G_t\langle\boldsymbol{J}_s\rangle\langle\boldsymbol{\omega}_g\rangle - G_g\langle\boldsymbol{J}_s\rangle\langle\boldsymbol{\omega}_t\rangle)\Omega
\end{aligned} \tag{24}$$

This control strategy requires the gimbal rate and gimbal accelerations to be chosen such that they satisfy Eq. (22). However, gimbal rates and accelerations are dynamically linked, so we cannot control them independently. Instead, we focus on the gimbal rates and make the assumption that the gimbal acceleration term is negligible with respect to the gimbal rate term. This leads to the reduced control law, which is shown in Eq. (25):

$$[D]\dot{\boldsymbol{\gamma}} \approx \boldsymbol{L}_r \tag{25}$$

With this reduced control law, the control strategy will focus on commanding gimbal rates while limiting gimbal acceleration. It is important to note that, for convergence, K must be a positive scalar and $[P]$ must be a symmetric positive definite matrix.

Next, the equation is rearranged to yield the desired gimbal rates. If $N = 3$ and the CMGs are not in gimbal lock (singular configuration), then a unique solution exists. Otherwise, a greater number of CMGs yields a null space that offers an infinity of solutions, which provides room for optimization. Generally, a minimum norm inverse is used to solve for the desired gimbal rates,

$$\dot{\boldsymbol{\gamma}}_{MN} = [D]^T([D][D]^T)^{-1}\boldsymbol{L}_r \tag{26}$$

Motor torques cannot instantaneously implement desired gimbal rates, so a subservo control loop is used to converge onto these desired rates. Using a similar Lyapunov analysis, we obtain a control in terms of gimbal accelerations as

$$\ddot{\boldsymbol{\gamma}} = -K_{\dot{\gamma}}(\dot{\boldsymbol{\gamma}} - \dot{\boldsymbol{\gamma}}_d) + \ddot{\boldsymbol{\gamma}}_d \tag{27}$$

The subscript d implies desired values that are obtained via the tracking control law. The desired gimbal accelerations must be determined numerically, or they may be ignored if a feedforward term is not important. For convergence, $K_{\dot{\gamma}}$ must be a positive scalar.

III. Power-Optimal Control Policy

To develop a power-optimal control law, it is necessary to first understand how power is related to the implemented control. Using the work-energy principle, the power equation for an N CMG spacecraft is shown in the following ([9] Chap. 4):

$$P = \boldsymbol{\omega}^T\boldsymbol{L} + \sum_{i=1}^{N}(\Omega_i u_{s,i} + \dot{\gamma}_i u_{g,i}) = \boldsymbol{\omega}^T\boldsymbol{L} + \boldsymbol{\Omega}^T\boldsymbol{u}_s + \dot{\boldsymbol{\gamma}}^T\boldsymbol{u}_g \tag{28}$$

$$\boldsymbol{u}_s = \langle\boldsymbol{J}_s\rangle G_s^T\dot{\boldsymbol{\omega}} + \langle\boldsymbol{J}_s\rangle\langle\boldsymbol{\omega}_t\rangle\dot{\boldsymbol{\gamma}} \tag{29}$$

Power is a function of the two rotation rates associated with a CMG (wheel rate and gimbal rate) and the torques associated with these rates. The gimbal torque is controlled for a CMG, but the spin torque is not actuated (it just maintains constant wheel speed). For this analysis, it is assumed that the external torque is independent of the desired gimbal rate.

This equation for power includes a term that we cannot instantaneously control, and that has no bearing on the control torques ($\boldsymbol{\omega}^T\boldsymbol{L}$). Additionally, this equation sums over the powers from each CMG to get a total value for the system. It is assumed that there is no system in place to reclaim power from the system when a negative power occurs (e.g., flywheel), so even when power reads as negative, the CMG must output energy. As such, it is necessary to adapt our power cost function to be more meaningful to this problem. Instead of minimizing the power equation shown previously, an analog that removes the term with no control torque and sums over the squares of the powers from the individual CMGs is used. This will ensure that the focus is on minimizing the magnitude of each of these powers rather than a sum in which a CMG with a strong negative power can negate the positive powers from the other CMGs. This power analogous function is defined as

$$\begin{aligned}
\mathcal{J}(\dot{\boldsymbol{\gamma}}) &= \frac{1}{2}\mathcal{P}^2 = \frac{1}{2}\boldsymbol{P}^T\boldsymbol{P} \\
\boldsymbol{P} &= (\langle\Omega\rangle\langle\boldsymbol{J}_s\rangle G_s^T + \langle\dot{\boldsymbol{\gamma}}\rangle\langle\boldsymbol{J}_g\rangle G_g^T)\dot{\boldsymbol{\omega}} \\
&\quad + (\langle\boldsymbol{J}_g\rangle\langle\ddot{\boldsymbol{\gamma}}\rangle - \langle\boldsymbol{J}_s - \boldsymbol{J}_t\rangle\langle\boldsymbol{\omega}_s\rangle\langle\boldsymbol{\omega}_t\rangle)\dot{\boldsymbol{\gamma}}
\end{aligned} \tag{30}$$

Other than minimizing this cost, it is important to also ensure that the control follows the tracking law and that it also does not require unachievable gimbal rates. As such, the equality constraint defined in Eq. (31) and the inequality constraint defined in Eq. (32) are enforced,

$$h(\dot{\boldsymbol{\gamma}}) = [D]\dot{\boldsymbol{\gamma}} - \boldsymbol{L}_r = 0 \tag{31}$$

$$g(\dot{\boldsymbol{\gamma}}) = \dot{\boldsymbol{\gamma}}^T\dot{\boldsymbol{\gamma}} - \dot{\gamma}_{\max}^2 \leq 0 \tag{32}$$

It should be noted that the maximum gimbal rate needs be set equal to or larger than the minimum norm solution since by definition this is the smallest gimbal rate that adheres to the tracking control law. Note that Eq. (31) is written to account for a general CMG steering law that requires $[D]\dot{\boldsymbol{\gamma}} = \boldsymbol{L}_r$, and the following general developments are not specific to the MRP-based attitude-tracking control employed in this study.

From this point, we will pursue a solution that minimizes this power analogous function while adhering to these two constraints. The problem is nonlinear in the control variable; thus, an analytical solution for N CMGs cannot be obtained; however, for a system with four CMGs, the problem can be solved explicitly. Both of these solutions will be explored in the following discussion.

A. Optimization for System with N CMGs

Minimization of this power-analogous cost function with an equality constraint and an inequality constraint is accomplished via application of the Karush–Kuhn–Tucker (KKT) conditions [12]. To apply these conditions, it is necessary to define the optimization Lagrangian function for this problem as

$$\mathcal{L}(\dot{\boldsymbol{\gamma}}, \boldsymbol{\lambda}, \mu) = \frac{1}{2}\mathcal{P}(\dot{\boldsymbol{\gamma}})^2 + \boldsymbol{\lambda}^T h(\dot{\boldsymbol{\gamma}}) + \mu g(\dot{\boldsymbol{\gamma}}) \tag{33}$$

The KKT conditions provide three necessary conditions for optimality (stationary, equality, and inequality conditions) as defined in Eqs. (34–36):

$$\frac{\partial \mathcal{L}(\dot{\boldsymbol{\gamma}}, \boldsymbol{\lambda}, \mu)^T}{\partial \dot{\boldsymbol{\gamma}}} = \frac{1}{2}\nabla \mathcal{P}(\dot{\boldsymbol{\gamma}})^2 + \nabla h(\dot{\boldsymbol{\gamma}})\boldsymbol{\lambda} + \mu \nabla g(\dot{\boldsymbol{\gamma}}) = 0 \tag{34}$$

$$h(\dot{\boldsymbol{\gamma}}) = 0 \tag{35}$$

$$\mu g(\dot{\boldsymbol{\gamma}}) = 0, \qquad \mu \geq 0 \tag{36}$$

The Lagrange multiplier on the inequality constraint μ can be viewed as a switching function, when exploring solutions in the domain where the constraint is negative the multiplier is zero, and on the boundary, the constraint acts as an equality constraint.

Evaluating each of the partial derivatives from Eq. (34), the results in Eqs. (37–39) are obtained:

$$\nabla \mathcal{P}(\dot{\boldsymbol{\gamma}})^2 = \frac{\partial \mathcal{P}^{2T}}{\partial \dot{\boldsymbol{\gamma}}} = 2\frac{\partial \boldsymbol{P}^T}{\partial \dot{\boldsymbol{\gamma}}}\boldsymbol{P} \tag{37}$$

$$\nabla h(\dot{\boldsymbol{\gamma}}) = \frac{\partial h(\dot{\boldsymbol{\gamma}})^T}{\partial \dot{\boldsymbol{\gamma}}} = [D]^T \tag{38}$$

$$\nabla g(\dot{\boldsymbol{\gamma}}) = \frac{\partial g(\dot{\boldsymbol{\gamma}})^T}{\partial \dot{\boldsymbol{\gamma}}} = 2\dot{\boldsymbol{\gamma}} \tag{39}$$

The partial derivative of the power-analogous function is nonlinear; thus, an explicit solution to this optimization problem cannot be obtained. Linearizing the problem to develop an iterative approach that converges on the nonlinear optimal solution provides a numerical method for solving the problem.

When linearizing, one cannot have discontinuities in the linearized parameters; thus, the solution must be approached in two ways: 1) optimize assuming the solution lies within the inequality constraint, and (if this solution is found to invalidate the inequality constraint) 2) optimize assuming $g(\dot{\boldsymbol{\gamma}})$ is an equality constraint. For the first approach, one must completely neglect the impact of the inequality constraint. Because the tracking constraint is linear in the control variable, it is not necessary to linearize with respect to the Lagrange multiplier, only with respect to the gimbal rates. This linearization is defined with respect to a nominal gimbal rate $\dot{\boldsymbol{\gamma}}^{(i)}$ as shown in Eq. (40), where the i superscript indicates the values on the ith iteration,

$$\frac{1}{2}[\nabla \mathcal{P}^2(\dot{\boldsymbol{\gamma}}^{(i)}) + \nabla^2 \mathcal{P}^2(\dot{\boldsymbol{\gamma}}^{(i)})\delta\dot{\boldsymbol{\gamma}}^{(i)}] + [D]^T\boldsymbol{\lambda}^{(i)} = 0 \tag{40}$$

Solving for the deviation in the gimbal rate from the nominal rate, one can substitute this into Eq. (35) to solve for the Lagrange multiplier in terms of the gimbal rate, which can in turn be used to solve explicitly for the linearized gimbal rate. The results of this process are defined in Eqs. (41) and (42). This process should be iterated until the gimbal rate update is less than a set tolerance ($\|\delta\dot{\boldsymbol{\gamma}}^{(i)}\|_\infty < \Delta$). In practice, starting with the minimum norm solution as the initial guess for this iterative root finder has been found to be effective at solving the problem,

$$\begin{aligned}\dot{\boldsymbol{\gamma}}^{(i+1)} &= \dot{\boldsymbol{\gamma}}^{(i)} + \delta\dot{\boldsymbol{\gamma}}^{(i)} \\ &= \dot{\boldsymbol{\gamma}}^{(i)} - (\nabla^2 \mathcal{P}^2(\dot{\boldsymbol{\gamma}}^{(i)}))^{-1}[2[D]^T\boldsymbol{\lambda}^{(i)} + \nabla \mathcal{P}^2(\dot{\boldsymbol{\gamma}}^{(i)})]\end{aligned} \tag{41}$$

$$\begin{aligned}\boldsymbol{\lambda}^{(i)} = -\frac{1}{2}&[[D](\nabla^2 \mathcal{P}^2(\dot{\boldsymbol{\gamma}}^{(i)}))^{-1}[D]^T]^{-1} \\ &\times [[D](\nabla^2 \mathcal{P}^2(\dot{\boldsymbol{\gamma}}^{(i)}))^{-1}\nabla \mathcal{P}^2(\dot{\boldsymbol{\gamma}}^{(i)}) - [[D]\dot{\boldsymbol{\gamma}}^{(i)} - \boldsymbol{L}_r]]\end{aligned} \tag{42}$$

If the solution to this problem does not satisfy the inequality constraint, the next step is to reoptimize now, assuming this constraint to be an equality constraint. Because this constraint is nonlinear in the gimbal rate, it is necessary to linearize with respect to its Lagrange multiplier. This linearization is defined in Eqs. (43) and (44):

$$\begin{aligned}&\frac{1}{2}[\nabla \mathcal{P}^2(\dot{\boldsymbol{\gamma}}^{(i)}) + \nabla^2 \mathcal{P}^2(\dot{\boldsymbol{\gamma}}^{(i)})\delta\dot{\boldsymbol{\gamma}}^{(i)}] + [D]^T\boldsymbol{\lambda}^{(i)} \\ &\quad + [\mu^{(i)}\nabla g(\dot{\boldsymbol{\gamma}}^{(i)}) + 2\mu^{(i)}\delta\dot{\boldsymbol{\gamma}}^{(i)} + \nabla g(\dot{\boldsymbol{\gamma}}^{(i)})\delta\mu^{(i)}] = 0\end{aligned} \tag{43}$$

$$(\dot{\boldsymbol{\gamma}}^{(i)^T}\dot{\boldsymbol{\gamma}}^{(i)} - \dot{\gamma}_{\max}^2) + 2\dot{\boldsymbol{\gamma}}^{(i)^T}\delta\dot{\boldsymbol{\gamma}}^{(i)} = 0 \tag{44}$$

Solving these equations along with the tracking equality constraint results in the linear solutions in Eqs. (45–49). Again, this process should be iterated until the desired level of convergence is achieved in both the gimbal rates and the inequality constraint Lagrange multiplier,

$$\begin{aligned}\dot{\boldsymbol{\gamma}}^{(i+1)} &= \dot{\boldsymbol{\gamma}}^{(i)} + \delta\dot{\boldsymbol{\gamma}}^{(i)} \\ &= \dot{\boldsymbol{\gamma}}^{(i)} - \left[\frac{1}{2}\nabla^2 \mathcal{P}^2(\dot{\boldsymbol{\gamma}}^{(i)}) + 2\mu^{(i)}I_{N\times N}\right]^{-1} \\ &\quad \left[\frac{1}{2}\nabla \mathcal{P}^2(\dot{\boldsymbol{\gamma}}^{(i)}) + \mu^{(i)}\nabla g(\dot{\boldsymbol{\gamma}}^{(i)}) + [D]^T\boldsymbol{\lambda}^{(i)} + \nabla g(\dot{\boldsymbol{\gamma}}^{(i)})\delta\mu^{(i)}\right]\end{aligned} \tag{45}$$

$$\mu^{(i+1)} = \mu^{(i)} + \delta\mu^{(i)} \tag{46}$$

$$\begin{bmatrix}\boldsymbol{\lambda}^{(i)} \\ \delta\mu^{(i)}\end{bmatrix} = Q^{-1}\boldsymbol{T} \tag{47}$$

$$Q = \begin{bmatrix}[D]\left[\frac{1}{2}\nabla^2 \mathcal{P}^2(\dot{\boldsymbol{\gamma}}^{(i)}) + 2\mu^{(i)}I_{N\times N}\right]^{-1} \\ 2\dot{\boldsymbol{\gamma}}^{(i)^T}\left[\frac{1}{2}\nabla^2 \mathcal{P}^2(\dot{\boldsymbol{\gamma}}^{(i)}) + 2\mu^{(i)}I_{N\times N}\right]^{-1}\end{bmatrix}\begin{bmatrix}[D]^T & \nabla g(\dot{\boldsymbol{\gamma}}^{(i)})\end{bmatrix} \tag{48}$$

$$\boldsymbol{T} = -\begin{bmatrix}[D]\\ 2\dot{\boldsymbol{\gamma}}^{(i)^T}\end{bmatrix}\left[\frac{1}{2}\nabla^2\mathcal{P}^2(\dot{\boldsymbol{\gamma}}^{(i)}) + 2\mu^{(i)}I_{N\times N}\right]^{-1} \times\left[\frac{1}{2}\nabla\mathcal{P}^2(\dot{\boldsymbol{\gamma}}^{(i)}) + \mu^{(i)}\nabla g(\dot{\boldsymbol{\gamma}}^{(i)})\right] + \begin{bmatrix}[D]\dot{\boldsymbol{\gamma}}^{(i)} - \boldsymbol{L}_r\\ \dot{\boldsymbol{\gamma}}^{(i)^T}\dot{\boldsymbol{\gamma}}^{(i)} - \dot{\gamma}_{\max}^2\end{bmatrix} \quad (49)$$

This method provides a solution that minimizes the power-analogous cost function subject to constraints that ensure the control still tracks the reference motion and does not command gimbal rates that are too large. The method works for $N > 3$ CMGs in the system but must be solved iteratively to obtain a control solution. The next subsection focuses on systems with $N = 4$ CMGs and how an analytical solution may be obtained for this specific case.

B. Optimization for a System with Four CMGs

Mechanical redundancy in space-based missions helps to prevent missions from early mechanical and electrical failures, and thus it is desirable; however, this must be balanced against the added mass and power requirements that redundant systems require. As such, a typical attitude control system has only four momentum exchange devices to provide the minimum amount of redundancy. Three are required for complete controllability, and the fourth provides the minimum amount of redundancy (assuming they are arranged properly to avoid gimbal lock). Our focus now is on obtaining an analytical solution to this problem for systems with four CMGs, since this would make the algorithm far more practically implementable for a real application.

In the previous method, tracking constraints were enforced via a Lagrange multiplier; however, given this is a linear constraint in the control, it can be implemented in an alternative manner. The $[D]$ matrix for a system with four CMGs has a defined null space that is one dimensional. The unit vector that defines this null space $\hat{n}$ is the unit eigenvector that accompanies the eigenvalue of zero for the matrix $[D]^T[D]$. If the solution to the gimbal rate is defined as described in Eq. (50), then the gimbal rate satisfies the tracking constraint for any real value of τ. The problem now is to select the parameter τ that minimizes the cost function subject to the defined inequality constraint,

$$\dot{\boldsymbol{\gamma}}(\tau) = \dot{\boldsymbol{\gamma}}_{MN} + \hat{n}\tau \quad (50)$$

To start this optimization process, the cost function is defined in terms of τ as shown in Eqs. (51–54):

$$\mathcal{J}(\tau) = \frac{1}{2}\mathcal{P}^2 = \frac{1}{2}\boldsymbol{P}_0^T\boldsymbol{P}_0 + \boldsymbol{P}_1^T\boldsymbol{P}_0\tau + \left(\boldsymbol{P}_2^T\boldsymbol{P}_0 + \frac{1}{2}\boldsymbol{P}_1^T\boldsymbol{P}_1\right)\tau^2 + \boldsymbol{P}_2^T\boldsymbol{P}_1\tau^3 + \frac{1}{2}\boldsymbol{P}_2^T\boldsymbol{P}_2\tau^4 \quad (51)$$

$$\boldsymbol{P}_0 = (\langle\boldsymbol{\Omega}\rangle\langle\boldsymbol{J}_s\rangle G_s^T + \langle\dot{\boldsymbol{\gamma}}_{MN}\rangle\langle\boldsymbol{J}_g\rangle G_g^T)[I]^{-1}[-\boldsymbol{\omega}\times[I]\boldsymbol{\omega} - A_{\dot{\gamma}}\dot{\boldsymbol{\gamma}}_{MN} - A_{\Omega}\boldsymbol{\Omega} - A_{\ddot{\gamma}}\ddot{\boldsymbol{\gamma}} + \boldsymbol{L}] + (\langle\boldsymbol{J}_g\rangle\langle\ddot{\boldsymbol{\gamma}}\rangle - \langle\boldsymbol{J}_s - \boldsymbol{J}_t\rangle\langle\boldsymbol{\omega}_s\rangle\langle\boldsymbol{\omega}_t\rangle)\dot{\boldsymbol{\gamma}}_{MN} \quad (52)$$

$$\boldsymbol{P}_1 = (\langle\boldsymbol{J}_g\rangle\langle\ddot{\boldsymbol{\gamma}}\rangle - \langle\boldsymbol{J}_s - \boldsymbol{J}_t\rangle\langle\boldsymbol{\omega}_s\rangle\langle\boldsymbol{\omega}_t\rangle)\hat{n} - (\langle\boldsymbol{\Omega}\rangle\langle\boldsymbol{J}_s\rangle G_s^T + \langle\dot{\boldsymbol{\gamma}}_{MN}\rangle\langle\boldsymbol{J}_g\rangle G_g^T)[I]^{-1}A_{\dot{\gamma}}\hat{n} + \langle\hat{n}\rangle\langle\boldsymbol{J}_g\rangle G_g^T[I]^{-1}[-\boldsymbol{\omega}\times[I]\boldsymbol{\omega} - A_{\dot{\gamma}}\dot{\boldsymbol{\gamma}}_{MN} - A_{\Omega}\boldsymbol{\Omega} - A_{\ddot{\gamma}}\ddot{\boldsymbol{\gamma}} + \boldsymbol{L}] \quad (53)$$

$$\boldsymbol{P}_2 = -\langle\hat{n}\rangle\langle\boldsymbol{J}_g\rangle G_g^T[I]^{-1}A_{\dot{\gamma}}\hat{n} \quad (54)$$

This results in a simple fourth-order polynomial cost function. To optimize this and obtain a solution, one simply needs to take the derivative of this polynomial and find the zeros of the resulting third-order polynomial [Eq. (55)], for which an analytic solution exists [13]:

$$\frac{\mathrm{d}\mathcal{J}(\tau)}{\mathrm{d}\tau} = \boldsymbol{P}_1^T\boldsymbol{P}_0 + (2\boldsymbol{P}_2^T\boldsymbol{P}_0 + \boldsymbol{P}_1^T\boldsymbol{P}_1)\tau + 3\boldsymbol{P}_2^T\boldsymbol{P}_1\tau^2 + 2\boldsymbol{P}_2^T\boldsymbol{P}_2\tau^3 = 0 \quad (55)$$

There will be three solutions to this minimization, but only real roots of the derivative that have positive second derivatives [Eq. (56)] can be minimizing solutions,

$$\frac{\mathrm{d}^2\mathcal{J}(\tau)}{\mathrm{d}\tau^2} = (2\boldsymbol{P}_2^T\boldsymbol{P}_0 + \boldsymbol{P}_1^T\boldsymbol{P}_1) + 6\boldsymbol{P}_2^T\boldsymbol{P}_1\tau + 6\boldsymbol{P}_2^T\boldsymbol{P}_2\tau^2 > 0 \quad (56)$$

In practice, only one of the three roots has been real with a positive second derivative (indicating a unique solution), but if a situation in which two plausible solutions exist arises, the one that gives a smaller cost function value or provides smaller commanded gimbal rates (if they are equal in cost) should be selected. It is easily shown that the solution is unique if and only if the following condition is satisfied:

$\Delta < 0$ and $a^2 > 0$, where

$$a = 2\boldsymbol{P}_2^T\boldsymbol{P}_2 \qquad b = 3\boldsymbol{P}_2^T\boldsymbol{P}_1 \qquad c = 2\boldsymbol{P}_2^T\boldsymbol{P}_0 + \boldsymbol{P}_1^T\boldsymbol{P}_1 \qquad d = \boldsymbol{P}_1^T\boldsymbol{P}_0$$

$$\Delta = 18abcd - 4b^3d + b^2c^2 - 4ac^3 - 27a^2d^2$$

If the resulting solution does not adhere to the inequality constraint, then the next step is to revaluate while using it as a new equality constraint [Eq. (57)]. This equation accounts for the fact that the null vector is orthogonal to the minimum norm solution by definition. This gives a quadratic equation in τ that is guaranteed to have two real solutions given that the maximum gimbal rates are not set lower than the minimum norm solution. One chooses the positive or negative root based on which yields a smaller cost function evaluation; this avoids having to solve for a Lagrange multiplier associated with this constraint,

$$\tau^2 + (\dot{\boldsymbol{\gamma}}_{MN}^T\dot{\boldsymbol{\gamma}}_{MN} - \dot{\gamma}_{\max}^2) = 0 \quad (57)$$

This fully defines our analytical power-optimal solution for systems with four CMGs. The method is easily implementable onboard a real spacecraft, requiring no integration or solution iteration, just accurate state estimates. For more complex systems, a power-optimal solution for N CMG systems is also derived. Although this solution requires iteration, it still provides a control with instantaneous power savings that asymptotically tracks a given reference motion. The following section provides an example of this algorithm at work and a discussion of how it compares to the minimum norm solution.

IV. Numerical Simulations

A numerical implementation of this policy is presented in this section. The results from the power-optimal policy are compared to the minimum norm solution to provide metrics for how these control policies perform. The minimum power is run at two different levels for the maximum gimbal rate in order to show how the inequality constraint affects the response. The first case sets the maximum at twice the minimum norm magnitude, and the second case sets it at four times the minimum norm magnitude. The test case presented here involves a spacecraft with four CMGs tracking the reference displayed in the following ($D = 1/1000$ s). Simulation parameters are defined in Tables 1–4. The initial

Table 1 System inertias

Inertia	Value, kg · m^2
$I_{S,1}$	86.215
$I_{S,2}$	85.070
$I_{S,3}$	113.565
J_{s_i}	0.130
J_{t_i}	0.040
J_{g_i}	0.030

Table 2 Initial states

State	Value
$\boldsymbol{\sigma}$	$[0.414, 0.3, 0.2]$
$B_{\omega_{B/N}}$, rad/s	$[0.01, 0.05, -0.01]$
Ω_i, rad/s	14.4
$\gamma_i(0)$, rad	0
$\dot{\boldsymbol{\gamma}}(0)$, rad/s	$[0, 0, 0, 0]$

Table 3 Initial CMG orientations

Axis	Values
$G_s(0)$	$\begin{bmatrix} 1 & -1 & 0 & 0 \\ 0 & 0 & 1 & -1 \\ 0 & 0 & 0 & 0 \end{bmatrix}$
$G_t(0)$	$\begin{bmatrix} 0 & 0 & -0.8166 & 0.8166 \\ 0.8166 & -0.8166 & 0 & 0 \\ -0.5771 & -0.5771 & 0.5771 & 0.5771 \end{bmatrix}$
$G_g(0)$	$\begin{bmatrix} 0 & 0 & 0.5771 & -0.5771 \\ 0.5771 & -0.5771 & 0 & 0 \\ 0.8166 & 0.8166 & 0.8166 & 0.8166 \end{bmatrix}$

Table 4 Control gains

Gain	Value
K, N · m	0.2
$K_{\dot{\gamma}}$, s^{-1}	1.5
$[P]$, N · m · s	$\begin{bmatrix} 3 & 0 & 0 \\ 0 & 3 & 0 \\ 0 & 0 & 3 \end{bmatrix}$

angular velocity and CMG orientations are defined with respect to the body fixed frame:

$$\boldsymbol{\sigma} = \begin{bmatrix} 2Dt \\ -(Dt)^2 \\ \frac{1}{2}Dt \end{bmatrix} \tag{58}$$

Figure 1 shows the convergence of the attitude and attitude rates of the simulation for each control law (body frame with respect to the reference motion). It is clear from these results that the two methods perform quite comparably over the entire simulation. At times, one performs slightly better than the other, but in general, no method is consistently dominant. This is to be expected since both control policies satisfy the tracking constraint that we derived. Given the same gains, both methods should converge at a comparable rate based on our Lyapunov analysis barring numerical errors in either method. The larger the maximum gimbal rate, the slower the convergence after 700 s, though. As such, it is recommended to switch to the minimum norm solution once the bulk of the convergence has been obtained since power savings are no longer a concern at such small torque levels, and the minimum norm solution performs better when subtle changes are needed since it requires smaller commanded gimbal rates as compared to the minimum power solutions.

The desired gimbal rates from all three simulations are summarized in Fig. 2. One might expect the minimum norm solution to have the smallest gimbal rates, but this is not the case. The highest peak gimbal rates occur for the minimum norm case, and as the maximum allowed gimbal rate is increased, that peak diminishes. This is because these control policies are optimal in an instantaneous sense, meaning they provide minimal solutions at the given time for a given set of states and control gains. Since these two solutions create two separate trajectories (with the same gains, but different states), there is no requirement that one must always provide a minimal gimbal rate or minimum power solution at all times. These optimal behaviors tend to pop out over the course of an entire simulation, but there will be times when the other solution performs better.

Having compared convergence and control results, it is now appropriate to compare performances based on the metric of interest in this paper, the power analogous cost function that was proposed [Eq. (30)]. These results are summarized in Fig. 3. It is clear in these results that the minimum power solution minimizes our cost function of interest in general, and it provides the best results as the maximum allowed gimbal rate is increased. Its peak power usage is smaller than the minimum norm solution for both cases, and there are periods in which it clearly outperforms the minimum norm solution (e.g., between 125 and 325 s). There are times when the minimum norm solution performs slightly better (especially in the turbulent periods when compared to the first minimum power simulation), but this is a symptom of the instantaneous nature of the optimization as discussed previously.

While this optimization procedure makes no guarantees about minimizing the cost across some duration, this might be expected since it guarantees optimal behavior at each instant. Figure 4 shows

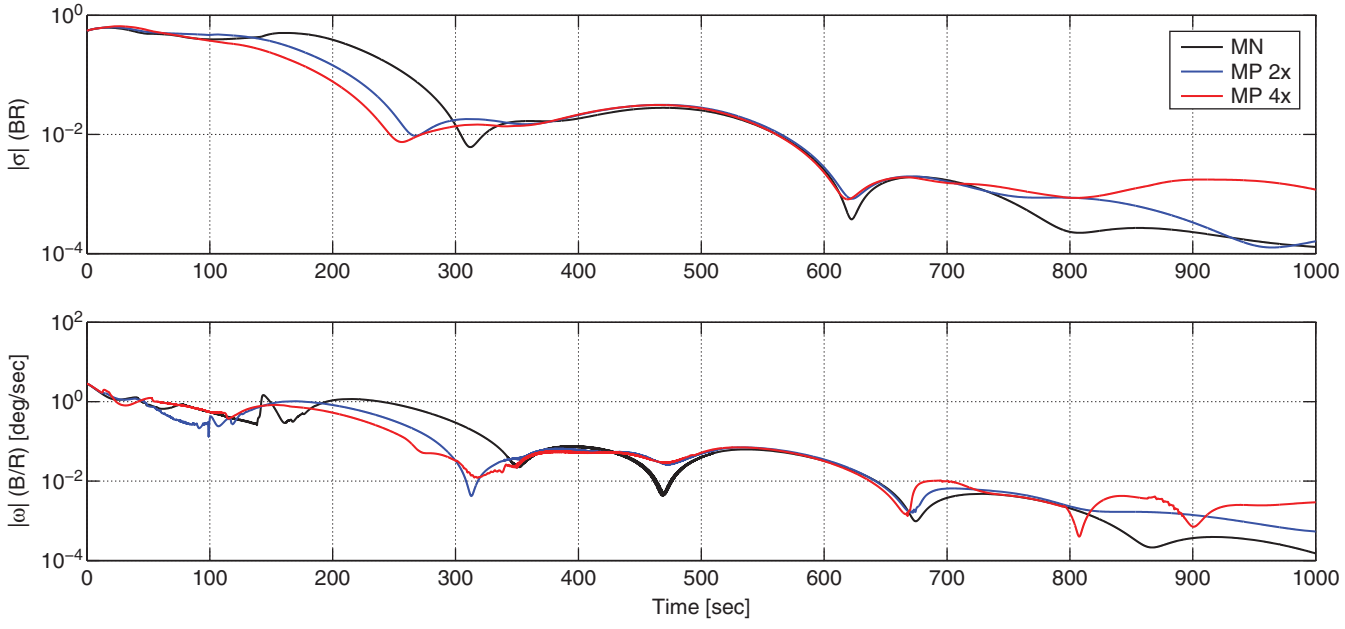

Fig. 1 Attitude (top) and attitude rate (bottom) convergence for each control law: (MN) minimum norm solution and (MP) minimum power solution.

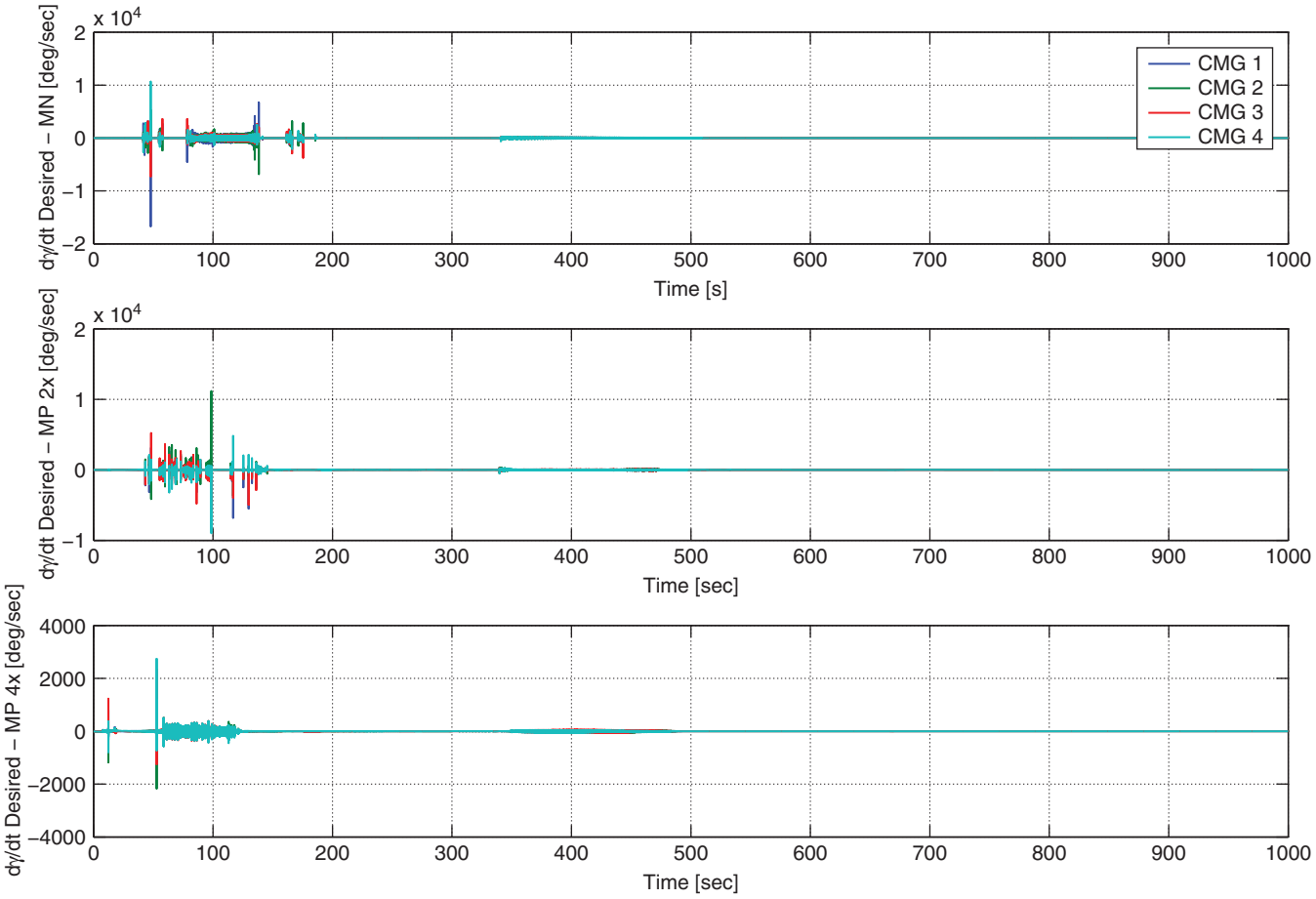

Fig. 2 Desired gimbal rates for each control law on their individual trajectories.

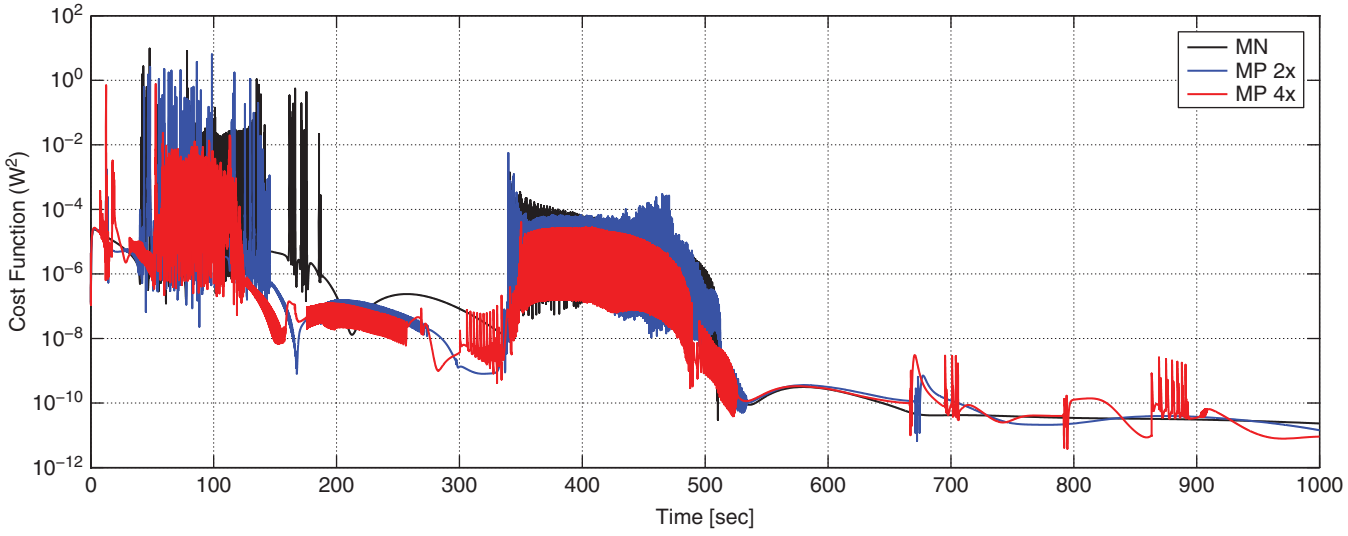

Fig. 3 Quadratic power analog for each control law on their respective trajectories.

the power-analogous cost function integrated with respect to time for all three cases. This integrated cost is similar to an energy metric (though the power was squared to make it positive definite), so it indicates how much energy the torques must impart on the system from the system's power subsystem. These results indicate that over the course of the maneuver the minimum power simulations outperform the minimum norm with total integrated costs that are 33% less and 92% less than the minimum norm's integrated cost, respectively. Both cases are significant power savings, but the latter is drastic. This demonstrates this algorithm's ability to save energy while providing comparable tracking performance when compared to the minimum norm solution. Furthermore, by adjusting system parameters such as gains and the maximum allowed gimbal rate magnitude (as demonstrated), it may be possible to find even greater energy savings. Such adjustments should be made before beginning any real attitude maneuver.

This simulation has demonstrated the minimum norm solution and this paper's minimum power solution as applied to a sample attitude-tracking scenario. It is clear from the results that both methods accurately track a reference motion and that the power-optimal solution tends to minimize power usage in the system with the drastic energy savings over the course of the entire simulation. This specific

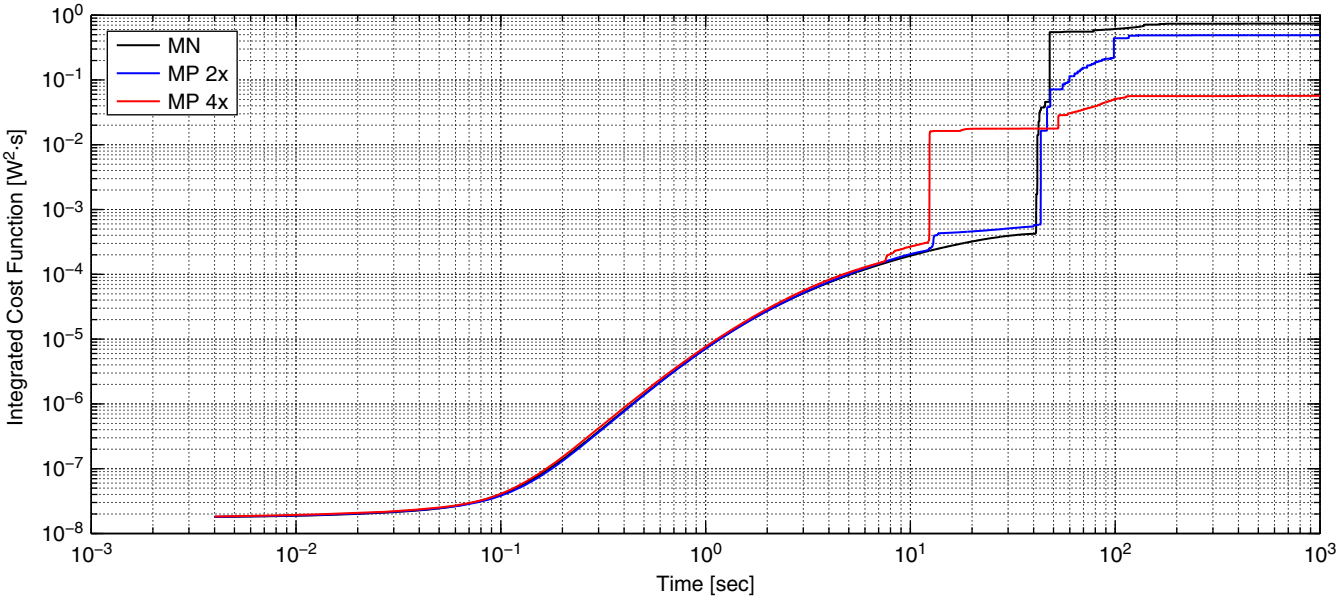

Fig. 4 Integrated cost function as a function of time for minimum norm and minimum power simulations.

example has some turbulent behavior that is a symptom of the system approaching gimbal lock. Without this issue, we would expect to see smoother behavior in the commanded gimbal rates and the power performance. In general, both methods should be simulated a priori and adjusted via gain selection in order to smooth out performance for actual implementation aboard a spacecraft.

V. Conclusions

This paper developed a new globally asymptotically stable tracking control policy that instantaneously optimized a power-analogous cost for systems with N control moment gyroscopes (CMGs). This development fills a hole by providing an instantaneous power-optimal infinite-horizon control policy for N CMG systems that is computationally simple to implement for real-time applications. The method developed may be solved via an iterative approach when the system has more than four CMGs, but for systems with four CMGs, an analytical solution was derived.

Through a numerical simulation, a comparison between the performance of this power-optimal policy and a more standard minimum norm solution was made. This revealed that both control policies accurately track a moving reference and that the optimal power policy minimizes power usage in the system, with the ability to yield drastic energy savings over the course of an entire maneuver. There are short periods in which the minimum norm solution performs slightly better, but overall the optimal solution performs better. Because these control policies are optimized instantaneously, there is no guarantee that the power-optimal solution will outperform the minimum norm solution for a given set of gains since they provide convergence via two separate state trajectories. As such, both methods should be tested a priori before large attitude maneuvers to determine which is best suited to be implemented and what the gains for the maneuver should be.

References

[1] Schaub, H., and Lappas, V. J., "Redundant Reaction Wheel Torque Distribution Yielding Instantaneous L_2 Power-Optimal Attitude Control," *Journal of Guidance, Control, and Dynamics*, Vol. 32, No. 4, Aug. 2009, pp. 1269–1276. doi:10.2514/1.41070

[2] Blenden, R., and Schaub, H., "Regenerative Power-Optimal Reaction Wheel Attitude Control," *Journal of Guidance, Control and Dynamics*, Vol. 35, No. 4, July–Aug. 2012, pp. 1208–1217. doi:10.2514/1.55493

[3] Dueri, D., Leve, F. A., and Acikmese, B., "Reaction Wheel Dissipative Power Reduction Control Allocation via Lexicographic Optimization," *AIAA/AAS Astrodynamics Specialist Conference*, AIAA Paper 2014-4103, 2014. doi:10.2514/6.2014-4103

[4] Richie, D. J., Lappas, V. J., and Palmer, P. L., "Sizing/Optimization of a Small Satellite Energy Storage and Attitude Control System," *Journal of Spacecraft and Rockets*, Vol. 44, No. 4, 2007, pp. 940–952. doi:10.2514/1.25134

[5] Lappas, V. J., Steyn, W. H., and Underwood, C., "Design and Testing of a Control Moment Gyroscope Cluster for Small Satellites," *Journal of Spacecraft and Rockets*, Vol. 42, No. 4, July–Aug. 2005, pp. 729–739. doi:10.2514/1.7308

[6] Leve, F. A., Boyarko, G. A., and Fitz-Coy, N. G., "Optimization in Choosing Gimbal Axis Orientations of a CMG Attitude Control System," *AIAA Infotech@Aerospace Conference*, AIAA Paper 2009-1836, 2009. doi:10.2514/6.2009-1836

[7] DeVon, D. A., Fuentes, R. J., and Fausz, J. L., "Passivity-Based Attitude Control for an Integrated Power and Attitude Control System Using Variable Speed Control Moment Gyroscopes," *Proceedings of the 2004 American Control Conference*, Vol. 2, IEEE, Boston, MA, June–July 2004, pp. 1019–1024.

[8] Carpenter, M. D., "Power-Optimal Steering of a Space Robotic System Driven by Control-Moment Gyroscopes," *AIAA Guidance, Navigation and Control Conference and Exhibit*, AIAA Paper 2008-7270, 2008. doi:10.2514/6.2008-7270

[9] Schaub, H., and Junkins, J. L., *Analytical Mechanics of Space Systems*, 3rd ed., AIAA Education Series, AIAA, Reston, VA, 2014, pp. 195–206

[10] LaSalle, J., and Lefschetz, S., *Stability by Lyapunov's Direct Method with Applications*, Academic Press, New York, 1961, pp. 56–70.

[11] Mukherjee, R., and Chen, D., "Asymptotic Stability Theorem for Autonomous Systems," *Journal of Guidance, Control, and Dynamics*, Vol. 16, No. 5, Sept. 1993, pp. 961–963. doi:10.2514/3.21108

[12] Kuhn, H. W., and Tucker, A. W., "Nonlinear Programming," *Proceedings of the Second Berkeley Symposium on Mathematical Statistics and Probability*, Univ. of California Press, Berkeley, CA, 1951, pp. 481–492.

[13] Press, W. H., Flannery, B. P., Teukolsky, S. A., and Vetterling, W. T., *Numerical Recipes in Fortran 77: The Art of Scientific Computing*, 2nd ed., Cambridge Univ. Press, Cambridge, England, U.K., 1992, pp. 362–371.